ISSN: 0067-2904

Morphological and Photometric Characteristics of Nearby Local Group Dwarf Galaxies

Layali Y. Salih AL-Mashhadani[1] , Ahmed H. Abdullah[2]
[1]*Department of Applied Mathematics, Mälardalen University, Sweden.*
[2]*Department of Astronomy and Space, College of Science, University of Baghdad, Baghdad, Iraq.*

Received:20/11/2024 Accepted: 23/3/2025 Published: 28/2/2026

Abstract

The morphological and photometric characteristics of dwarf galaxies in the local group are key to understanding galaxy structure and evolution, providing insight into the properties of low-luminosity systems. However, their faint nature makes them challenging to observe, especially at greater distances. In this study, we examined the morphological classification, spatial distribution, and photometric properties of a sample of 33 nearby dwarf galaxies at approximately 2 kpc, using data from the Sloan Digital Sky Survey (SDSS-IV) data release 18 (DR18), to investigate how these galaxies are varying in terms of their colors, surface brightness, and structural features.

Our results reveal notable trends in the relationship between morphology and distance for dwarf irregular (dIrr) and dwarf spheroidal (dSph) galaxies. We observe that dIrr galaxies are more dispersed and commonly found at greater distances, additionally, they are gas-rich galaxies with recent star formation, while dSph galaxies contain older stellar populations and tend to cluster closer to their host galaxies like the Miley Way. In general, we noticed that the dSph galaxies appear redder and fainter due to the intermediate and old age stars, and the containment of metal-rich stars, whereas the dIrr galaxies tend to be bluer and brighter, indicating the presence of younger stars which contain fewer heavy elements.

Keywords: Dwarf galaxies, local group, photometric galaxy morphology, redshift.

الخصائص المورفولوجية والضوئيّة للمجرات الأقزام القريبة في المجموعة المحلية

ليالي يحيى صالح[1] , أحمد حسن عبد الله[2]*
[1]قسم الرياضيات التطبيقية، جامعة مالاردالن، السويد
[2] قسم الفلك والفضاء، كلية العلوم، جامعة بغداد، بغداد، العراق

الخلاصه

تُعتبر الخصائص الشكلية و الضوئيّة للمجرات الأقزام في المجموعة المحلية أساساً لفهم تطوير المجرات، مما يوفر نظرة ثاقبة لخصائص الأنظمة منخفضة اللمعان. ولكن من الصعب رصدها، وبالأخص على مسافات بعيدة بسبب طبيعتها الخافتة.

*Email: ahmed.h.abdullah@sc.uobaghdad.edu.iq

في هذه الدراسة، قمنا بفحص التصنيف الشكلي، التوزيع المكاني، والخصائص الضوئية لعينة من المجرات الأقزام القريبة والمتكونة من ٣٣ مجرة تقع على مسافة ٢ كيلو فرسخ فلكي تقريبا، باستخدام بيانات من الماسح الرقمي للسماء والمعروف عالميا باسم(Sloan Digital Sky Survey)
تكشف النتائج عن اتجاهات واضحة في العلاقة بين الشكل والمسافة بالنسبة لكل من المجرات الأقزام غير المنتظمة dIrr والمجرات الأقزام الكروية الشكل .dSph حيث لاحظنا ان المجرات الأقزام غير المنتظمة كانت أكثر انتشاراً وغالبا ماتكون متواجدة على مسافات بعيدة وتتميز بتكوين نجمي حديث، إضافة إلى انها غنية بالغازات. بينما تحتوي المجرات الأقزام الكروية على تجمعات نجمية قديمة وتميل إلى التكتل بالقرب من المجرات المضيفة. وعلى العموم لاحظنا ان المجرات الكروية تبدو أكثر احمراراً بسبب النجوم متوسطة العمر والقديمة، واحتواء النجوم الغنية بالمعادن، في حين ان المجرات الأقزام غير المنتظمة تميل إلى ان تكون أكثر زرقة، مما يشير إلى وجود نجوم أصغر سنا واحتوائها على القليل من العناصر الثقيلة.

1. Introduction

Satellite galaxies (SGs) are compact stellar systems, usually containing millions of stars, that are frequently found within the gravitational pull of bigger host galaxies, like the Milky Way (MW). Often labeled as dwarf galaxies due to their significantly smaller size compared to their primary counterparts, these systems are vital for piecing together the puzzle of galactic behavior and development. Exploring them sheds light on the mechanisms driving galaxy formation, as well as the hierarchical assembly of cosmic structures [1]

Dwarf galaxies exist in a variety of shapes and sizes, each providing important insights into the forces that influence galaxy evolution. Generally, group them into three main categories: dwarf spheroidal (dSph), dwarf irregular (dIrr), and dwarf elliptical (dE) galaxies [2,3]. The dIrr type stands out with its rich gas reserves, active star birth, and appears blue resulting from a dynamic group of young, hot stars. In contrast, dSph and dE galaxies generally lack gas, predominantly containing older stars and exhibiting smooth, elliptical forms. This results in a reddish appearance and lower luminosity when compared to their irregular counterparts [4,5].

Dwarf galaxies display distinct photometric characteristics—such as brightness, color, and surface brightness—that significantly contribute to understanding their composition and historical evolution [6]. Among these, dIrr galaxies are known to exhibit greater luminosity and show bluer colors, indicating that star formation is still occurring. In contrast, dSph galaxies tend to be dimmer and exhibit redder colors, suggesting the presence of an older stellar population [7]. To analyze their stellar content and chemical evolution, astronomers often rely on the color-magnitude diagram (CMD), which helps in identifying patterns in their formation and evolutionary processes [8].

Research has been conducted about the observational properties of dwarf galaxies in the local group (LG), e.g. [6, 7]. Kormendy [3] demonstrated that two relations appear to arise, one for "giant" galaxies and the other for "dwarf" galaxies when elliptical galaxies' surface brightness is plotted against luminosity. This has typically been read as proof that both systems belong to two different groups. The discrepancy in the origin of dE and E galaxies has been one of the interesting topics for years. A popular argument is that E galaxies were released quickly during a prominent starburst at the very beginning of the universe and were formed via a scenario known as monolithic collapse [8]. Ultra-compact dwarf galaxies and dSphs have a striking difference in the mass-radius relation and an imbalance of the galaxy's evolution. This can be translated into the conditions through which these galaxies were formed [9, 10, 11].

The majority of the galaxies in the universe are dwarf galaxies [1]. These systems are almost too faint to be detected for high redshifts. Nevertheless, in the local group, we get a clear picture of the early star formation and chemical enrichment of these galaxies. The LG of galaxies concentrates on the massive spiral galaxies, MW and M31, each hosting an amount of smaller satellite dwarf galaxies with mass smaller than $10^{9.5}$ M_sun [12] and luminous less than −17 mag, in the V-band [7]. Sawala et al. [13] demonstrated that all satellites of MW reside within a thin plane by studying the spatial distribution of eleven MW satellites. Metz et al. [14] show that the disk of satellites of the Milky Way is inclined with respect to the supergalactic plane. More studies confirmed the existence of planar distribution for MW satellite spatial distribution [14, 15]. The spatial distribution of the SG is correlated with the larger-scale filamentary pattern [16, 17,18]. Tully et al. [18] claimed the existence of two nearly parallel satellite planes. They suggested that the plane around the MW is not aligned with the cosmic web while it is mainly aligned around M31 [20, 21]. The spatial distribution of the M31 satellite galaxies has been investigated. Santos S. al. [22] found a vast thin plane of satellites around M31.

The environment of the galaxies has a severe impact on their evolution and hence influences their physical characteristics. This is relevant due to dwarf galaxies being more vulnerable to the effects of nearby galaxies that are more massive due to their low total masses.

The goal of this project is to explore the morphological and photometric properties of dwarf galaxies within the local group. Our aim is to investigate the relationship between the morphological classification of the galaxies and distance to examine their spatial distribution in the local group. On the other hand, this study aims to review the fundamental photometric properties of the dwarf galaxies in the local group and to understand the galaxies' formation and valuation.

2. Data Collection

In this study, we collected data samples of 33 dwarf galaxies in the local group: dwarf irregular galaxies (dIrr), and dwarf spherical galaxies (dSph), using data from the Sloan Digital Sky Survey (SDSS-IV) Data releases 18 (DR18) at https://www.sdss.org/dr18/, and NASA/IPAC Extragalactic Database (NED) at http://ned.ipac.caltech.edu.

We selected data about the redshift measurements, galactic coordinates such as the galactic latitude and the galactic longitude, morphological type of each galaxy, as well as the photometric data, typically the absolute magnitude in V-band, (B-V) color index, surface brightness, and the half-light radius. The obtained data were in FITs format which is commonly used in astronomy. We then used R (programming language), along with the “fitso” package, to process the data and extract the important properties that were needed in the analysis and visualizations. The fundamental properties of the studied samples of 33 galaxies are shown in Table 1. Table 1 displays: galaxy’s name, heliocentric redshift (zhelio), angular diameter in arcsec (Ad), half-light radius in arcmin, and location of the galaxies according to the galactic latitude/ galactic longitude, and the absolute magnitude Mv.

Table 1: Fundamental properties of the studied dwarf galaxies

Name (1)	z_Helio (2)	Type (3)	*v*_Helio (4)	Ad (5)	Rh (6)	G_lat. (7)	G_long. (8)	Mv (9)	Distance (10)
IC10	-0.00116	dIrr	-348.0590	809.40	2.65	-3.327392	119.0	-19.3	825
IC1613	-0.00078	dIrr	-234.1379	1320.00	6.81	-60.577318	129.8	-15.1	700
LGS 3	-0.00096	dIrr/dSph	-286.6016	-	2.10	-40.893880	126.8	-10.08	810
Phoenix	0.00013	dIrr	39.872402	457.09	3.76	-65.721999	272.2	-23.99	445
Leo I	0.00095	dSph	285.1026	720.0	3.40	49.112412	240.16	-11.84	250
Sextans A	0.00108	dIrr	324.0756	353.3	2.47	39.875583	233.2	-14.6	1440
Sextans I	0.00075	dSph	224.244790	-	-	42.272386	21.1	-9.23	86
Sextans B	0.00100	dIrr	300.991670	360.0	1.06	43.783826	25.3	-14.9	1345
Leo II	0.00026	dSph	79.1452	900.0	2.60	67.231269	34.0	-9.7	205
SagDIG	-0.00026	dIrr	-78.5456	210.0	0.91	-16.287940	322.9	-11.5	1060
NGC 6822	-0.00018	dIrr	-54.8620	1117.30	2.65	-18.399152	11.9	-15.2	490
DDO 210	-0.00047	dIrr	-140.0030	157.80	1.47	-31.343098	75.9	-12.4	800
Tucana	0.00065	dIrr	193.9657	173.00	1.10	47.369300	196.9	-9.53	880
UKS2323-326	0.00021	dIrr	62.0570	201.84	0.90	-70.858916	11.867	-13.24	1320
WLM	-0.00041	dIrr	-122.3153	704.90	7.78	10.42	5.6	-14.5	925
NGC 147	-0.00064	dE/dSph	-193.0663	900.00	3.17	-14.252616	119.8174	-15.1	725
NGC 185	-0.00067	dE/dSph	-202.0601	929.30	2.25	-14.482456	120.791	-15.8	620
NGC 205	-0.00080	dE/dSph	-241.0331	1312.70	2.46	-21.138755	120.7	-16.5	815
Carina	0.00070	dSph	223.045620	1800.00	8.20	-22.223423	343.9	-9.08	101
Leo A	0.00007	dIrr	20.086098	330.00	2.15	52.422527	310.7	-12.8	101
Ursa Minor	-0.00082	dSph	-247.0290	2400.00	8.20	44.800397	144.7	-8.67	66
Draco	-0.00098	dSph	-294.995820	3000.0	10	34.721827	226.0	-8.93	82

M32	-0.00071	Ce	-212.8526	660.00	0.47	-21.976158	121.1	-16.5	805
Fornax A	0.00018	dSph	53.363065	4200.00	16.6	-56.690021	243.49	-13.2	138
Pegasus II	-0.00114	dSph	-340.8640	-	2.10	-36.324541	220.17	-11.42	955
Antlia	0.00121	dIrr	362.1493	125.40	1.2	22.312406	260.1	-11.5	1235
Sagittarius	0.00047	dIrr	140.0030	-	0.91	-16.287940	105.0	-13.61	24
NGC 55	0.00044	dSph	131.0093	2290.87	5.16	-	86.37	-18.0	1480
IC 5152	0.00041	dIrr	122.0155	431.52	0.97	-50.191810	240.16	-18.2	1590
GR 8	0.00071	dIrr	214.0518	66.00	0.32	76.979424	94.8	-11.9	1590
And II	-0.00065	dSph	-193.6659	-	6.20	-29.161142	332.7	-12.36	525
And III	-0.00115	dSph	-344.1617	-	2.20	-26.264272	128.9	-9.96	760
And I	-0.00126	dSph	-376.2395	-	3.10	-24.816535	119.37	-11.75	805
EGB 0427+63	-0.00033	dIrr	-98.931525	203.30	-	-	144.7	-12.6	1300

3. Data processing

To ensure our dataset was accurate and complete, we first checked for any missing or corrupted R-studio Data Recover Software was used to rover and clean the dataset, making sure all values were correct and ready for analysis. Each galaxy's position was initially recorded in the equatorial coordinate system (right ascension, declination). Since our study focuses on the Milky Way, we converted these coordinates into the galactic coordinate system (longitude, latitude) using standard transformation equations. This conversation helped us analyze the spatial distribution of these galaxies relative to the Milky Way. The transformation is outlined in Binney & Merrifield (1998) [23].

$$\sin b = \sin\delta \cos b_{NGP} - \cos\delta \sin b_{NGP} \cos(\alpha - \alpha_{NGP}) \quad (1)$$

$$\cos b \sin(l - l_{NGP}) = \cos\delta \sin(\alpha - \alpha_{NGP}) \quad (2)$$

$$\sin b \cos(l - l_{NGP}) = \sin\delta \sin b_{NGP} + \cos\delta \cos b_{NGP} \cos(\alpha - \alpha_{NGP}) \quad (3)$$

Where (α, δ) are the equatorial coordinates (Right Ascension, Declination), and (I, b) are the Galactic coordinates (longitude and latitude). The reference parameters for the transformation are ($\alpha_{NGP} = 192.85948^o$, $b_{NGP} = 27.12825^o$) for the North Galactic Pole (NGP) and $l_{NGP} = 122.932^o$ for the Galactic longitude of the North Celestial Pole.

Once the coordinates were transformed, we used R-studio software to analyze the spatial distribution of the galaxies using the Cumulative Distribution Function CDF for both dwarf irregular (dIrr) and dwarf spheroidal (dSph) galaxies, allowing us to compare their spatial distributions and identify trends. Finally, R-studio was also used for data visualization. We

created spatial distribution maps, velocity distance plots, and color-magnitude diagrams, which helped us interpret the physical and photometric properties of the galaxies in our sample.

4. Results and Discussion

4.1 Distribution of the dIrr and dSph in galactic coordinates

A comparison of the spatial distribution of dwarf galaxies and their morphological trends is shown in Figure 1. As illustrated in the figure, the dIrr galaxies are widely spread, and located farther from massive galaxies such the Andromeda (M31) and Milky Way, which indicates that they are less gravitationally, and are influenced by external interactions. dSph galaxies are more located around massive galaxies, which suggests that these galaxies are affected by a stronger gravitational influence.

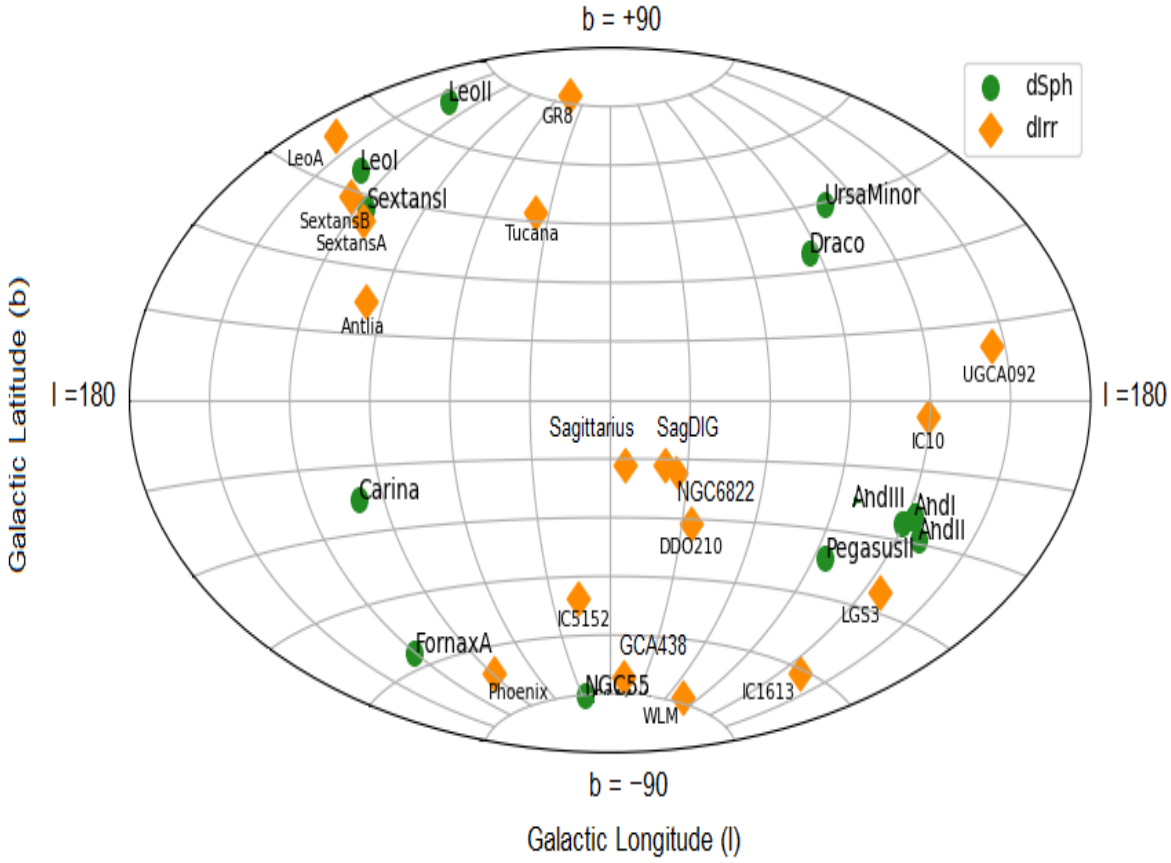

Figure 1: Distribution of local group dwarf galaxies in Galactic coordinates for the heliocentric redshift range of $-1 \times 10^{-3} < z < 1 \times 10^{3}$.

The difference in the distribution in galactic coordinates of the dIrr and dSph galaxies is shown in Figures 2 and 3. Figure 2 shows the distribution of the dIrr galaxies in the galactic longitude/ latitude against the heliocentric redshift (z_{helio}). As we can see, the tendency follows a more scattered and diagonal distribution which emphasizes that they are more affected by external forces such as the tidal interaction in the local group [24, 25]. This confirms the dispersed structure of dIrr galaxies, reinforcing their lower gravitational binding and irregular motion [26]. Unlike dIrr galaxies, the distribution of the dSph galaxies appears more evenly spread without a diagonal trending, as illustrated in Figure 3. Instead, their distribution is clustering in specific regions showing a broad spatial spread below and above the galactic plane. Instead, it reveals clustering in specific regions, likely due to past

interactions with the Milky Way, which has significantly shaped their orbits and structural properties [26].

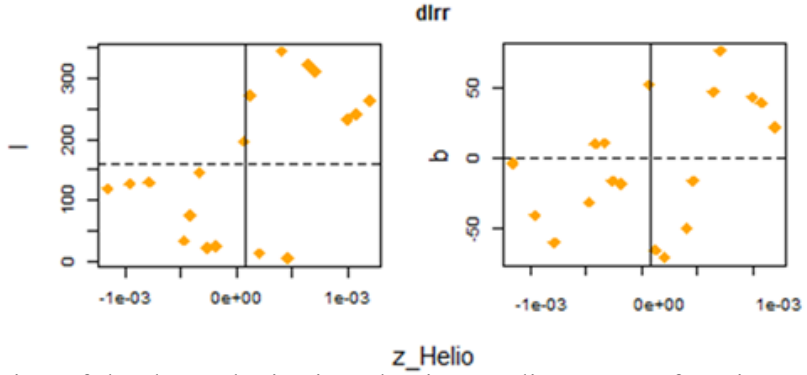

Figure 2: Distribution of the dIrr galaxies in galactic coordinates as a function to z_{helio} . Left panel: in galactic longitude (l). Right panel: in galactic longitude (b)

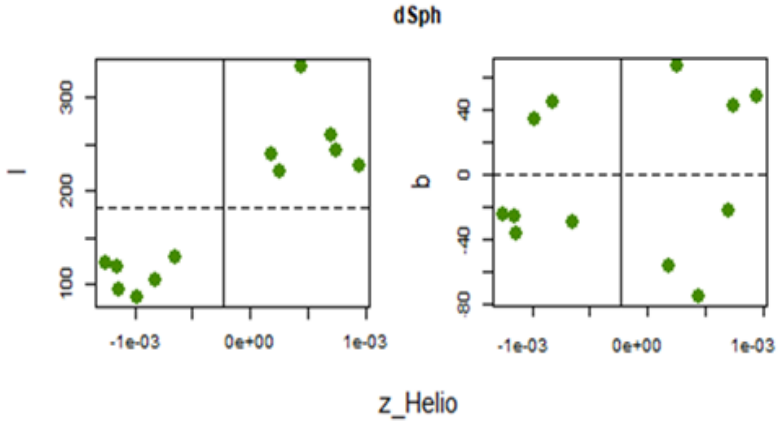

Figure 3: Distribution of the dSph galaxies in galactic coordinates as a function to z_{helio} . Left panel: in galactic longitude (l). Right panel: in galactic longitude (b)

4.2 Cumulative distribution of dIrr and dSph

We depend on the cumulative distribution function (CDF) for each type of galaxy to create cumulative distribution plots of dwarf irregular galaxies (dIrr) and dwarf spheroidal galaxies (dSph).

The distributions for the Satellite galaxies (dIrr and dSph) are shown in Figure (4a). The distribution is clearly non-uniform and shows a strong preference for |cos (θ)| around 40. The colored region (box) shows where they are most concentrated, i.e. within any range relative to latitude. The dIrr type is more frequent than the dSph (see Figure 4b).

In Figure 5, the apparent magnitude values for dwarf irregular galaxies are notably higher than those for dwarf spheroidal galaxies. The figure includes an overlaid orange curve, which represents a smoothed kernel density estimate. The mean absolute magnitudes, indicated by vertical blue lines, are measured at 11.71 mag for dIrr galaxies and 10.4 mag for dSph galaxies. This difference can be explained by the fact that dIrr galaxies are gas-rich and continue to undergo active star formation [28, 29, 30].

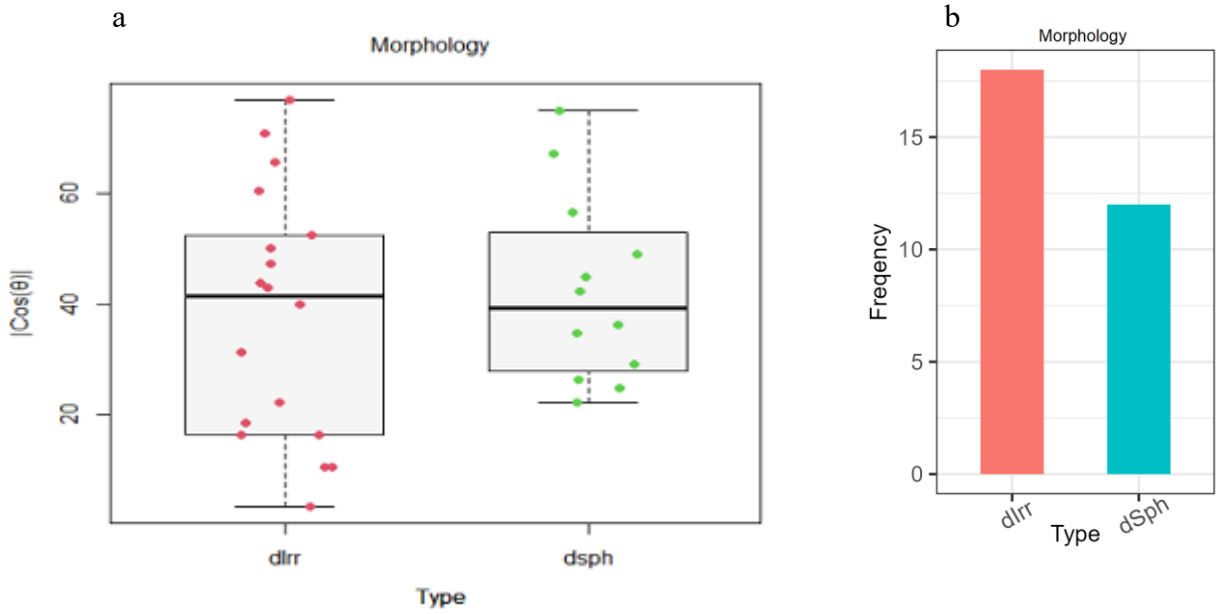

Figure 4: a) The cumulative distribution of the galaxies as a function of |cos (θ)| where θ is Galactic latitude. b) the frequency of each galaxy type, indicating a higher count of dIrr galaxies in the sample.

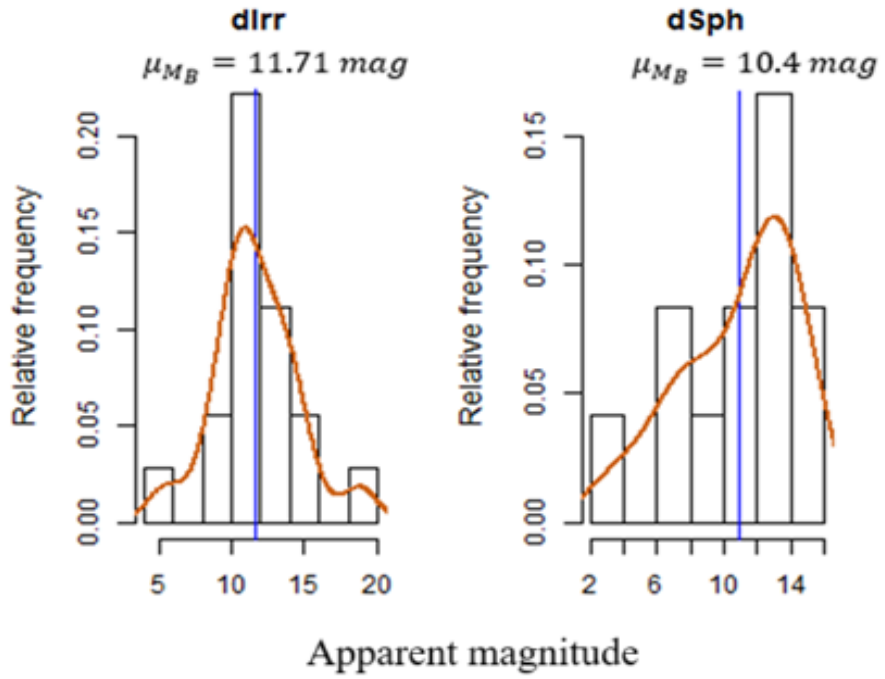

Figure 5: Distribution of apparent magnitudes for irregular dwarf galaxies (dIrr) and dwarf spheroidal galaxies (dSph).

4.3 Velocity distribution and circular velocity curves of simulated dwarf galaxies analyzed using the R programming language

This section explores the motion of dwarf galaxies in the local group and their interactions with larger galaxies like the Milky Way and Andromeda.

Figure 6 shows the velocity-distance diagram for galaxies across three distance regions. In this first region (0.024-0.5 Mpc), velocity ranges widely from -295 km /s to + 28, reflecting complex Dynamics like gravitational interactions and orbital motion. Some galaxies move toward the Milky Way, while others move away. In the second region (0.5-1 Mpc), most

galaxies have negative velocities, suggesting motion toward the Milky Way or local group's center. However, Tucana stands out with a positive velocity, possibly due to a unique orbit or peculiar motion. The third region (1-1.59 Mpc) shows velocities from -98.93 km/s to +105.7 km/s, indicating weaker Milky Way influence and more independent motion within the local group [25].

Figure 7 illustrates the link between heliocentric velocity and cos(θ), where θ is galactic latitude. The dashed line shows the best-fit model for $v = v(\cos(\theta))$. A strong correlation would suggest that galaxy motion is due to the Milky Way's gravity or local group dynamics. Deviations from the fit indicate that these galaxies have deviant velocities, likely from past interactions, tidal effects, or their gradual infall into the local group [27].

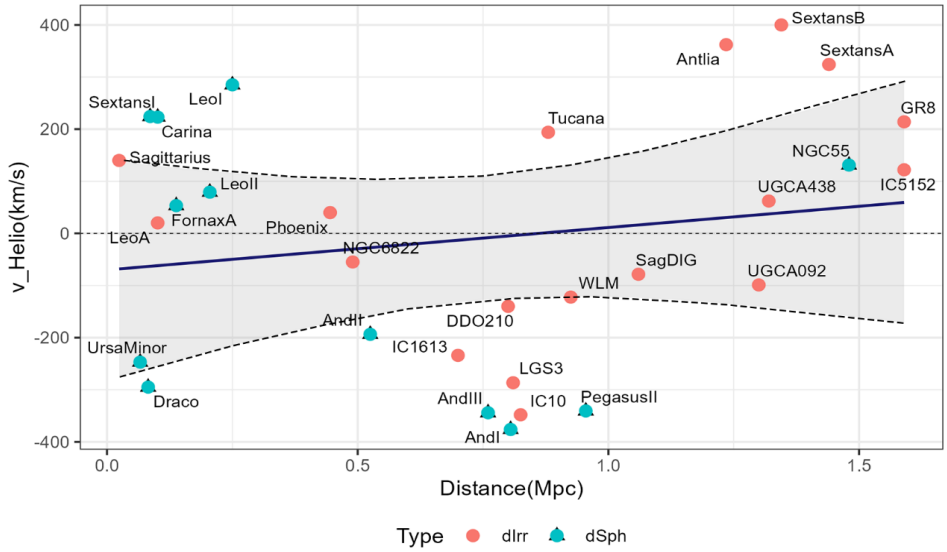

Figure 6: Velocity-distance diagram for the galaxies at distances larger than 1.5 Mpc.

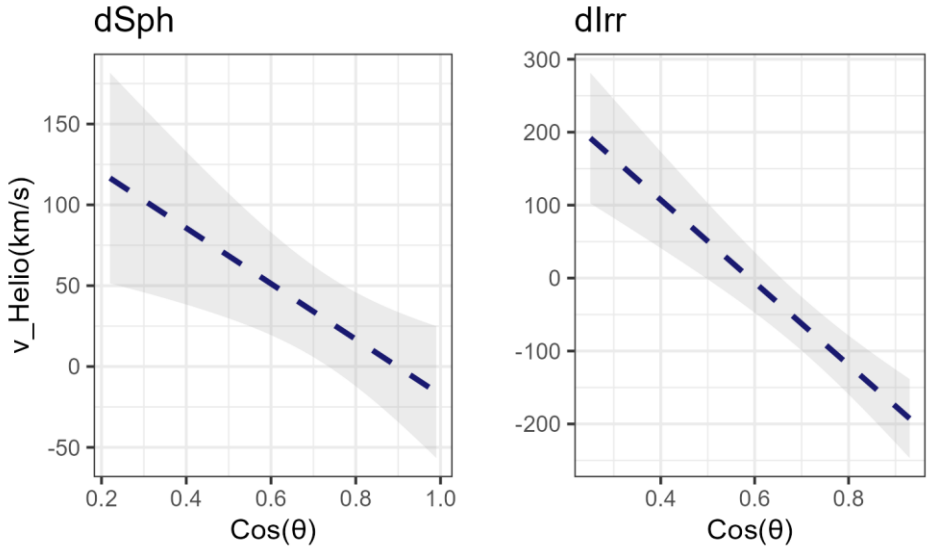

Figure 7: Heliocentric velocities of the galaxies as a function of cos(θ). The dashed line indicated the best fit to the $v = v(cos\ (\theta))$ relation.

4.4 Color index and Surface brightness

4.4.1 Colors

Color-magnitude diagram of the galaxy sample is presented in Figure 8 which shows the (B-V) color index versus the absolute magnitude in the V-band. The absolute magnitude Mv for dwarf spherical galaxies (dSph) on the left panel in Figure 8 ranges between -8.67 to -18.0 mag, while the Mv range of the dwarf irregular galaxies (dIrr) on the right panel varies from -9.53 to -23.99 mag. The color index distribution of the dIrr galaxies is more scattered in comparison with the dSph galaxies. Some of the dIrr galaxies exhibit noticeable deviations from the dashed trend line in the figure and are trending slightly downward. In contrast, the dSph galaxies are trending upwards.

Figure 8 also shows that the dSph galaxies seem to be brighter and tend to be redder B-V values close to 1, indicating older galaxies, more evolved stellar populations, and contain metal-rich stars. Meanwhile, the dIrr galaxies have bluer B-V values close to 0.4-0.6, which indicate the presence of younger stars that contain fewer heavy elements and ongoing star formation.

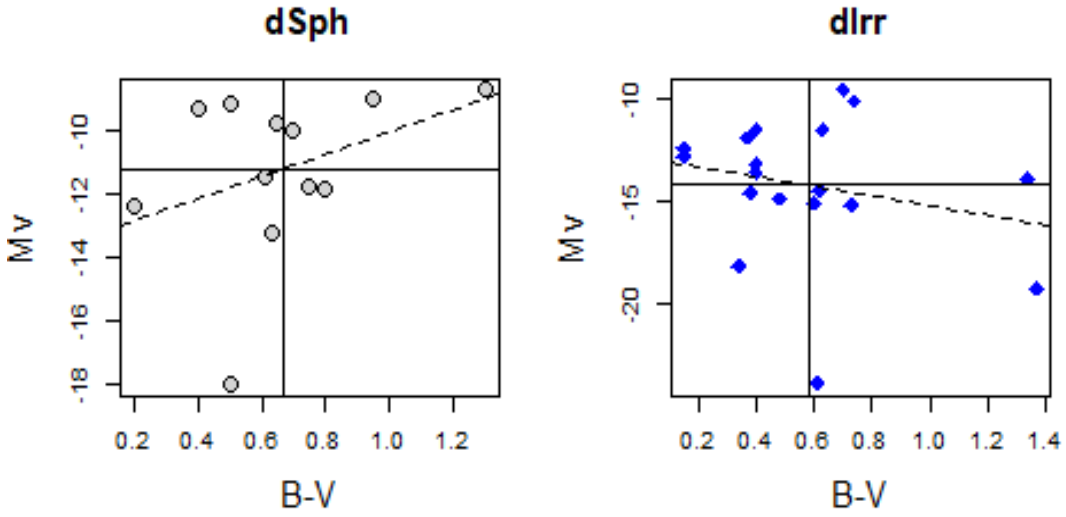

Figure 8; The color-magnitude diagram of the sample is based on the (B-V) colors of the galaxies and the absolute magnitudes in the V-band.

Figure 9, illustrates histograms of B-V colors for the dSph galaxies (left panel) and dIrr galaxies (right panel), the vertical blue line provides the mean B-V values. The figure shows that dIrr galaxies reveal a wider variety of colors, with a peak in the blue region of a mean value of 0.68 mag, reflecting younger stellar populations and active star formation. On the other hand, the dSph galaxies have a narrower color distribution toward the redder region, with a mean value of 0.58 mag showing they are redder than dIrr and older.

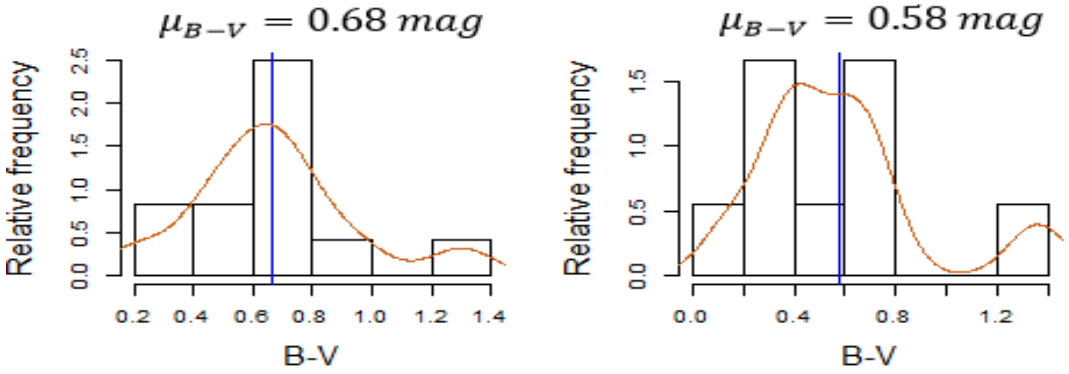

Figure 9: The histogram of B-V colors of dIrr and dSph galaxies on the left and right respectively. The vertical blue line shows the mean value.

4.4.2 Surface brightness

Figure 10 presents the surface brightness of the galaxies in the sample against the absolute magnitude. The diagonal solid line in the figure explores the tendency of constant surface brightness, calculated by the averaging values within the half-light radius. The dIrr and dSph galaxies that spread along the diagonal line have various brightness levels indicating variations in the star formation history and stellar populations. Notably, brighter galaxies tend to gather closer to this line, illustrating a correlation between the surface brightness and the absolute magnitude Mv. Generally, the dIrr galaxies seem to be fainter than dSph galaxies.
Figure 11 provides the relationship between the absolute magnitude in V-band ranging from -23 to -5 versus the half-light radius for the sample. The half-light radii of the dIrr galaxies on the left panel range between (0.32-7.78) arcmin whereas the dSph on the right panel spans with a larger range (3-17) arcmin. Figure 11 highlights the dIrr galaxies exhibit lower half-light radii at higher magnitudes, reflecting their irregular morphology and active star formation. While the dSph have larger half-light radii at fainter magnitudes indicating extended and diffuse structures.

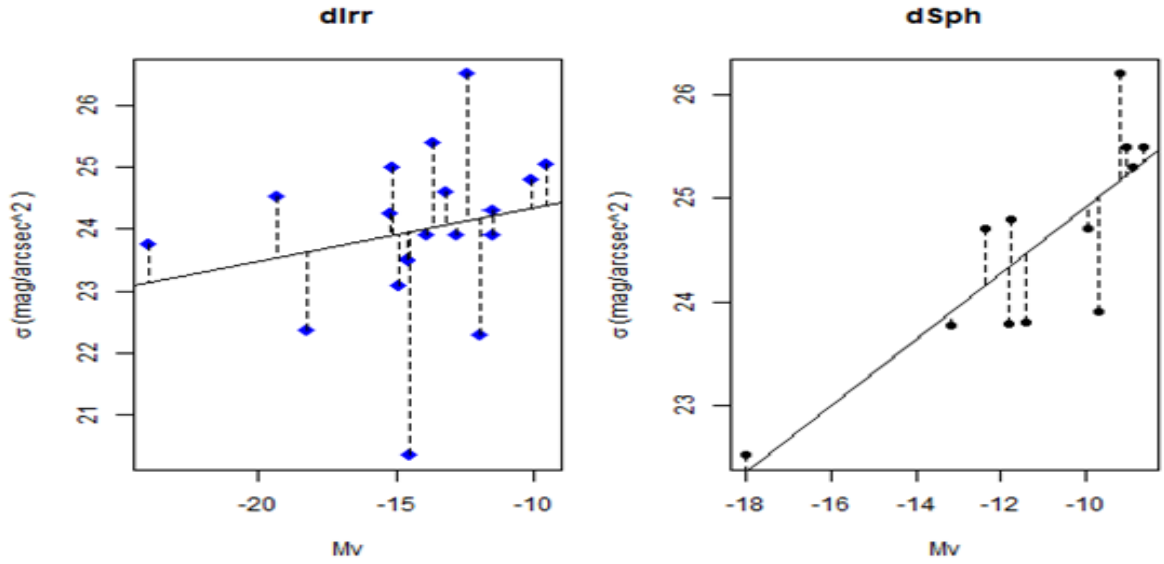

Figure 10: The surface brightness versus absolute magnitude. The diagonal solid line represents the direction determined by (averaged within the half-light radius) points of constant surface brightness.

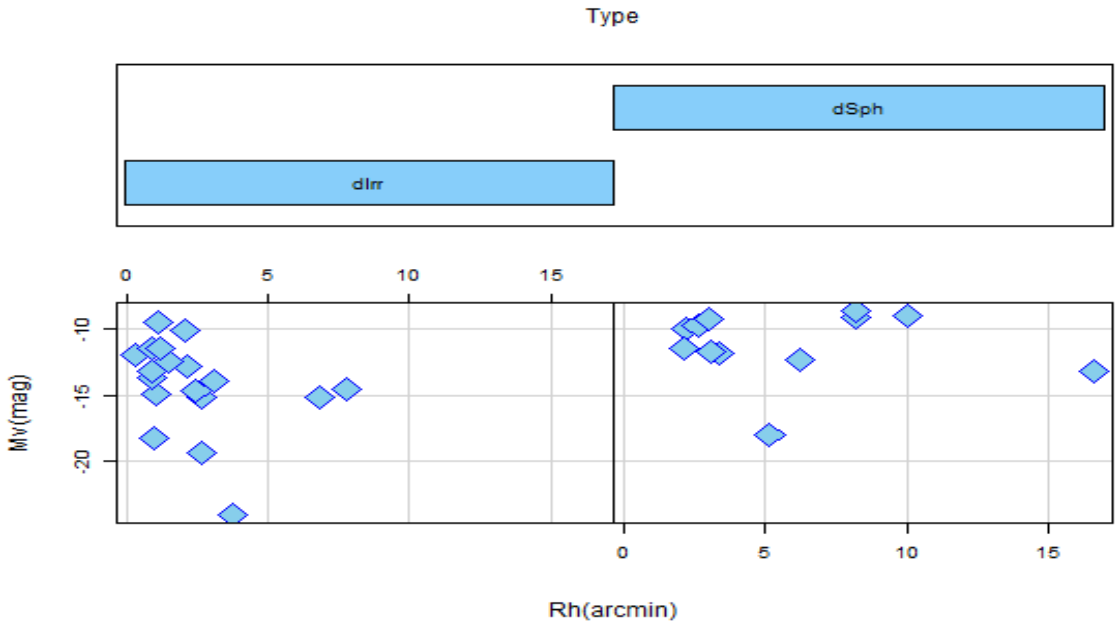

Figure 11: The absolute magnitude versus half-light radius for the galaxy sample around $-23 \leq M_v \leq -5$ for dIrr and dSph galaxies on the left and right respectively

5. Conclusions

Dwarf galaxies, regarded as the foundational components of massive galaxies, rank among the faintest entities in the universe. This research has investigated the known satellite systems of the Milky Way (MW) and Andromeda (M31) galaxies, as well as semi-isolated systems within the local group. Our primary focus was on the morphological and photometric attributes of nearby dwarf galaxies, particularly the irregular (dIrr) and dwarf spheroidal (dSph) types.

We have examined various physical properties, including the positions, structures, and dynamical traits of these satellite dwarf galaxies. Our results reveal notable differences between dIrr and dSph galaxies when compared. dlrr galaxies tend to be widely distributed and are typically found at higher galactic longitudes. In contrast, the dSph galaxies cluster closer to massive galaxies like the Milky Way. In addition, the dIrr galaxies have higher values of absolute magnitude due to their gas-rich nature and active star formation, while dSph galaxies appear fainter and redder and contain older stars.

The cumulative distribution function (CDF) analysis reveals that the distribution of the dIrr and dSph galaxies are non-uniform, hence, the dIrr are more concentrated in specific latitude regions and are more frequent than dSph galaxies. Moreover, analysis of the distribution of the dIrr and dSph on the velocity-distance diagram identifies three distinct regions based on galaxy motion. Within the 0.024 to 0.5 Mpc range, dIrr galaxies exhibit both positive and negative velocities, whereas dSph galaxies predominantly show negative velocities in the 0.5 - 1 Mpc range. This distinction suggests different dynamical influences and evolutionary pathways.

References

[1] K. Wang, "An evolutionary continuum from nucleated dwarf galaxies to star clusters," *Nature*, vol. 623, no. 7986, pp. 296–300, 2023. doi:10.1038/s41586-023-06650-z.

[2] M. Seo and H. B. Ann, "Star formation histories of dwarf spheroidal and dwarf elliptical galaxies in the local Universe," *Monthly Notices of the Royal Astronomical Society*, vol. 520, no. 4, pp. 5521–5535, 2023. doi:10.1093/mnras/stad425.

[3] J. Kormendy, "Structure and Evolution of Dwarf Galaxies," in *Lessons from the Local Group: A Conference in Honor of David Block and Bruce Elmegreen*, vol. 323, 2015, p. 323. doi: 10.1007/978-3-319-10614-4_27.

[4] S. Mau, "Two Ultra-faint Milky Way Stellar Systems Discovered in Early Data from the DECam Local Volume Exploration Survey," *The Astrophysical Journal*, vol. 890, no. 2, Art. no. 136, 2020. doi: 10.3847/1538-4357/ab6c67.

[5] O. Müller et al., "The properties of dwarf spheroidal galaxies in the Cen A group: Stellar populations, internal dynamics, and a heart-shaped Hα ring," *Astron. Astrophys.*, vol. 645, p. A92, Jan. 2021. doi:10.1051/0004-6361/202039359.

[6] C. Olsen and E. Gawiser, "Searching for Conformity Across Cosmic Time with Local Group and Local Volume Star Formation Histories," *The Astrophysical Journal*, vol. 943, no. 1, Art. no. 30, 2023. doi: 10.3847/1538-4357/acaa39.

[7] A. Fattahi, J. F. Navarro, and C. S. Frenk, "The missing dwarf galaxies of the Local Group," *Monthly Notices of the Royal Astronomical Society*, vol. 493, no. 2, pp. 2596–2605, 2020. doi: 0.1093/mnras/staa375.

[8] L. Y. S. Al-Mashhadani and A. H. Abdullah, "A cosmological view for the time-variation of the fundamental constants of nature," *NeuroQuantology*, vol. 18, no. 12, 2020. doi: 10.14704/nq.2020.18.12.NQ20233

[9] T. Saifollahi, J. Janz, R. F. Peletier, et al., "Ultra-compact dwarfs beyond the centre of the Fornax galaxy cluster: hints of UCD formation in low-density environments," *Monthly Notices of the Royal Astronomical Society*, vol. 504, no. 3, pp. 3580–3609, 2021. doi: 0.1093/mnras/stab1118.

[10] A. H. Abdullah and P. Kroupa, "The Dichotomy of the Mass-radius Relation and the Number of Globular Clusters," *Astronomy Letters*, vol. 47, pp. 170–174, 2021. doi: 10.1134/S1063773721030014.

[11] D. K. A. and M. N. Al Najm, "Investigation of the Characteristics of CO (1-0) Line Integrated Emission Intensity in Extragalactic Spirals," *Iraqi Journal of Science*, vol. 63, no. 3, pp. 1376–1393, Mar. 2022. doi: 10.24996/ijs.2022.63.3.39.

[12] J.-B. Salomon, N. Libeskind, and Y. Hoffman, "Exploring the centre of mass properties of LG-like galaxies," *Monthly Notices of the Royal Astronomical Society*, vol. 523, no. 2, pp. 2759–2769, 2023. doi: 10.1093/mnras/stad1598.

[13] T. Sawala et al., "The Milky Way's plane of satellites is consistent with Λ CDM," *Nature Astronomy*, vol. 7, no. 4, pp. 481–491, 2023. doi: 10.48550/arXiv.2205.02860.

[14] M. Metz, P. Kroupa, and H. Jerjen, "The spatial distribution of the Milky Way and Andromeda satellite galaxies," *Monthly Notices of the Royal Astronomical Society*, vol. 374, no. 3, pp. 1125–1145, 2022. doi: 10.1111/j.1365-2966.2006.11228.x.

[15] A. Eckart et al., "The infrared K-band identification of the DSO/G2 source from VLT and Keck data," *Proceedings of the International Astronomical Union*," vol. 9, no. S303, pp. 269–273, 2013. doi: 10.1017/S1743921314000726.

[16] Q. Gu, "The spatial distribution of satellites in galaxy clusters," *Monthly Notices of the Royal Astronomical Society*, vol. 514, no. 1, pp. 390–402, 2022. doi: 10.1093/mnras/stac1292.

[17] L. Tang, W. Lin, and Y. Wang, "Satellite Alignment. III. Satellite Galaxies' Spatial Distribution and Their Dependence on Redshift with a Novel Galaxy Finder," *The Astrophysical Journal*, vol. 893, no. 2, Art. no. 87, 2020. doi: 10.3847/1538-4357/ab8292.

[18] R. B. Tully, N. I. Libeskind, and I. D. Karachentsev, "Two planes of satellites in the Centaurus A group," *The Astrophysical Journal Letters*, vol. 802, no. 2, Art. no. L25, 2015. doi: 10.1088/2041-8205/802/2/L25.

[19] N. Fernando et al., "On the stability of satellite planes - I. Effects of mass, velocity, halo shape and alignment," *Monthly Notices of the Royal Astronomical Society*, vol. 465, no. 1, pp. 641–652, 2022. doi: 10.1093/mnras/stw2694.

[20] M. A. Aragon-Calvo, J. Silk, and M. Neyrinck, "The unusual Milky Way-local sheet system: implications for spin strength and alignment," *Monthly Notices of the Royal Astronomical Society: Letters*, vol. 520, no. 1, pp. L28–L32, Mar. 2023. doi: 10.1093/mnrasl/slac161.

[21] I. M. Santos-Santos, R. Domínguez-Tenreiro, and M. S. Pawlowski, "An updated detailed characterization of planes of satellites in the MW and M31," *Monthly Notices of the Royal Astronomical Society*, vol. 499, no. 3, pp. 3755–3774, 2020. doi: 10.1093/mnras/staa3130.

[22] M. P. Rey et al., "EDGE: from quiescent to gas-rich to star-forming low-mass dwarf galaxies," *Monthly Notices of the Royal Astronomical Society*, vol. 497, no. 2, pp. 1508–1520, 2020. doi: 10.1093/mnras/staa1640

[23] J. Binney and M. Merrifield, *Galactic Astronomy*. Princeton, NJ, USA: Princeton University Press, 1998.

[24] M. Mateo, "Dwarf Galaxies of the Local Group," *Annu. Rev. Astron. Astrophys.*, vol. 36, pp. 435–506, 1998. doi: 10.1146/annurev.astro.36.1.435.

[25] A. W. McConnachine, "The observed properties of dwarf galaxies in and around the Local Group," The Astronomical Journal, vol. 144, no. 1, p. 4, 2012. doi:10.1088/0004-6256/144/1/4.

[26] J. Gensior and J. M. D. Kruijssen, "The elephant in the bathtub: when the physics of star formation regulate the baryon cycle of galaxies," *Monthly Notices of the Royal Astronomical Society*, vol. 500, no. 2, pp. 2000–2011, 2021. doi: 10.1093/mnras/staa3453.

[27] E. K. Grebel, "Evolutionary Histories of Dwarf Galaxies in the Local Group," *The Stellar Content of the Local Group*, IAU Symposium 192, pp. 17-38, 1999. doi: 10.1017/S0074180900203884.

[28] H. R. Al-Baqir and A. K. Ahmed, "Explaining the photometric and spectroscopic properties of The Sip-39 galaxy pair," *Baghdad Science Journal*, vol. 21, no. 4, pp. 1403–1415, 2024. doi: 10.21123/bsj.2023.8316.

[29] N. Fukagawa,"Star formation and gas flow history of a dwarf irregular galaxy traced by gas-phase and stellar metallicities," Monthly Notices of the Royal Astronomical Society, vol. 491, no. 2, pp. 1759–1770, 2020. doi: 10.1093/mnras/stz3104.

[30] M. N. Al Najm, A. H. Abdullah, and Y. E. Rashed, "Estimating the evolution and the content fractions of baryonic gas for Luminous Infrared Galaxies," Mon. Not. R. Astron. Soc., vol. 537, no. 2, pp. 1597–1607, 2025. doi: 10.1093/mnras/staf023.